THERMAL PARAMETERS ANALYSIS DURING DIRECTIONAL SOLIDIFICATION OF Al-Cu EUTECTIC ALLOYS

Alex Ivan Kociubczyk[1], Federico Cabello[2], Carlos Enrique Schvezov [1,2], Ricardo Walter Gregorutti[3], Alicia Esther Ares [1,2]
[1] Materials Institute of Misiones, IMAM (CONICET-UNaM), University of Misiones, 1552 Azara Street, (3300) Posadas, Argentina.
[2] Member of CIC of the National Research Council (CONICET) of Argentina.
[3] Researcher at LEMIT– CIC. Engineering Faculty. National University of La Plata.

Keywords: Aluminum-Copper alloys, Columnar-to-equiaxed transition, Solidification parameters, Structural parameters.

Abstract

Al-Cu eutectic alloy samples (Al-33.2wt.%Cu) were solidified directionally upward under conditions which produce the columnar-to-equiaxed transition (CET) phenomenon.
The position of the CET was located in each sample and the distance from the bottom of the ingot was measured. During solidification the distribution of temperatures were measured by means of thermocouples located strategically. From the measured temperatures the following parameters were obtained; local temperature gradient, cooling rate of the liquid and solid and growth rate. Three different velocities of heat extraction were employed and the temperature gradient reaches values of 2.1 ºC/cm, 0.1 °C/cm and -4.3ºC/cm, , respectively. The results are presented and discussed comparing with the results obtained in the case of CET in dendritic Al-Cu alloys

Introduction

In general, the columnar-to-equiaxed transition, CET, occurs when the equiaxed grains are sufficient in size and number to impede the advance of columnar front. The extent of the equiaxed zone is the result of competition between columnar and equiaxed grains [1-5].
As a liquid is cooled at the eutectic composition, the two phases grow simultaneously as an interconnected structure which forms the solid eutectic phase. The phase has a lamellar structure, which consists of many thin alternating layers of the two components.
The lamellar structure ensures that there are very small diffusion fields head of the solid-liquid interface, meaning that atoms do not travel over very significant distances for the two phases to simultaneously form.
The eutectic lamellae shows the co-operative formation of θ and Al (α) phases. The SEM picture in Figure 1 shows an interlamellar spacing of about 1 μm, as well as some imperfections which form from irregularities and disturbances during growth.

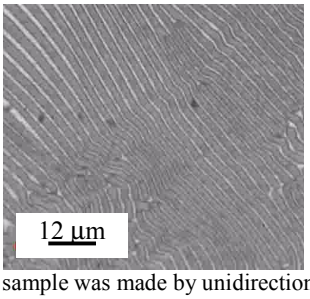

Figure 1. This sample was made by unidirectional cooling and was metallographically prepared

Eutectic growth stability depends on the degree of cooling of the solid / liquid interface [6-19], that is, the difference between the eutectic temperature, T_E, and the temperature of the interface, T_I. Eutectic growth in lamellar or fibrous, the two phases, α and β, cooperatively grow side by side, with a solid / (S / L) liquid interface next to be flat and with a total supercooling, ΔT. The accumulation of solute interfacial with lateral diffusion during growth interfacial decreases temperature to below the eutectic temperature in an amount ΔT_C. This contribution to the total supercooling due to the difference in composition between the local composition $C_{\alpha,\beta}(X)$ and the eutectic composition C_E. Furthermore, the curvature of the thermal drift occurs in relation to the temperature of a planar interface, resulting in the contribution, ΔT_σ , in complete supercooling. Ultimately, ΔT_k, is the contribution to the kinetic supercooling. Total supercooling, ΔT, in a certain place of the interface is given by the sum of: $\Delta T_C + \Delta T_\sigma \Delta T_k$. The kinetic supercooling, is negligible in non-faceted systems. Thus, it is assumed that the total supercooling in the interface is given by:

$$\Delta T = \Delta T_E - \Delta T_I = \Delta T_C + \Delta T_\sigma \quad (1)$$

Based on suggestions from Brandt, Zener and Hillert Tiller [37], Jackson and Hunt [38] assumed that the total supercooling should be constant. This is equivalent to writing:

$$\Delta T_{\alpha,\beta} = \Delta T_C + \Delta T_\sigma = m_{\alpha,\beta}\left[C_E - C_{\alpha,\beta}(x)\right] + \frac{a^L_{\alpha,\beta}}{R_{\alpha,\beta}(x)} = cte \quad (2)$$

where a is a constant given by the ratio of Gibbs-Thomson, $R_{\alpha,\beta}(x)$ is the local curvature of the interface, $m_{\alpha,\beta}$ is the inclination of the lines of each α and β, C(x) liquidus phase, is the composition at point x and the upper index L denotes lamellar concerning growth values.
a and R (x) constants, corresponding to the local temperature variations in balance in relation to the eutectic temperature and can be derived from the thermodynamic equilibrium systems, establishing an equality between the chemical potentials.

Total average supercooling of each phase at the interface for a lamellar eutectic is obtained by solving the diffusion equation. Jackson and Hunt got that expression equal to:

$$\Delta T_\alpha = m_\alpha\left[C_\infty + B_0 + 2\frac{V}{D}C_0\frac{(S_\alpha + S_\beta)^2}{S_\alpha}P\right] + \frac{a_\alpha{}^L}{S_\alpha} \quad (3)$$

$$\Delta T_\beta = m_\beta \left[-C_\infty - B_0 + 2\frac{V}{D} C_0 \frac{(S_\alpha + S_\beta)^2}{S_\beta} P \right] + \frac{a_\beta^L}{S_\beta} \quad (4)$$

with:

$$a_\alpha^L = \left(\frac{T_E}{L_f}\right)_\alpha \sigma_\alpha^L \text{sen}\theta_\alpha^L \quad \text{and} \quad a_\beta^L = \left(\frac{T_E}{L_f}\right)_\beta \sigma_\beta^L \text{sen}\theta_\beta^L$$

L_f parameter is the latent heat of fusion per unit of volume of each phase, σ_α *and* σ_β are the surface tensions between the liquid and α and β phases, respectively. Equations (2) and (3) contain three variables: λ, V and ΔT. The relationship between them can be better addressed using what is referred to as growth agreed in extreme conditions, where the total should be minimal supercooling for a given growth rate [21] Under these conditions there is a minimum for a constant growth rate found in the solution of the equations (2) and (3), that is, the eutectic increases according to

$$\lambda^2 V = \frac{a^L}{Q^L} = \text{Cons tan te} \quad (5)$$

The relationship obtained in extreme conditions, corresponds to one of the most interesting and important results of the theory of Jackson and Hunt [12]. According to Trivedi et al. [6, 13, 14], the approaches used with low speed, can not be applied when growth occurs at high solidification rates, or rapid solidification processes. Trivedi also states that for all values of k, the model provides for a maximum speed above which no further growth of cooperative eutectic phases is observed.

According to Aziz [15], when the advance of the interface occurs with much higher speeds than the diffusion rate, the solute atoms are encompassed by the interface and included in the solid progression, which can result in amorphous regions of solidified structure, a phenomenon known as solute trapping.

While all these works have significantly contributed from different aspects to understanding the phenomenon of the CET, there are no sufficient data in the literature about detailed measurements of thermal and metallographic parameters in a specific alloy system (eutectic composition).

The objective of the present work was to generate detailed experimental data of thermal (cooling rate, temperature gradient, solidification velocity) and metallographic (grain size and eutectic spacing) parameters during directional solidification of aluminum–copper eutectic (Al-33.2 wt%Cu) alloys with the CET.

Experimental

Al-Cu Eutectic alloys (33.2wt.%Cu) provided by Arcolana® were solidified directionally upwards in an experimental setup consisting on a heat unit, a temperature control system, a temperature data acquisition system, a sample moving system and a heat extraction system (Figure 2).

During solidification process, temperatures at different positions in the alloy samples were measured. For the measurements a set of five thermocouples arranged was used. The thermocouples were of the K type (1.8 mm). The thermocouples were previously calibrated using four temperature points; demineralized water at the freezing and boiling points (corrected by atmospheric pressure), and aluminum and Al-Cu eutectic alloy at their fusion points. During solidification experiment, the temperature measured by each thermocouple was recorded at regular intervals of time of 0.5 seconds using.

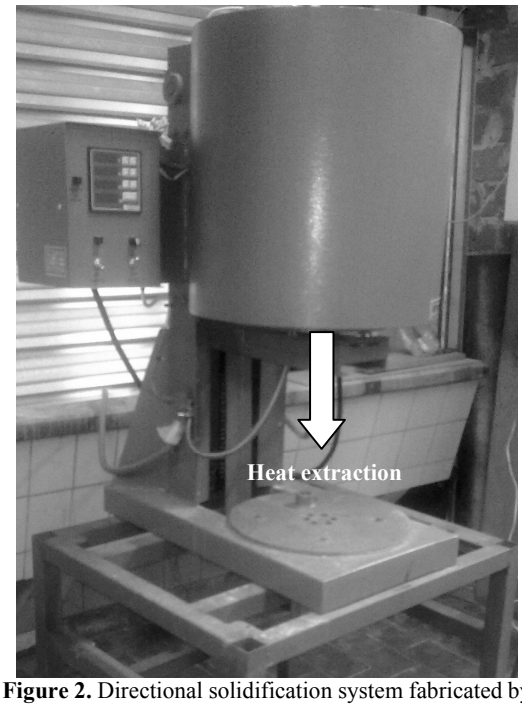

Figure 2. Directional solidification system fabricated by Hornos Estigia®, La Plata, Argentina.

The eutectic alloys directionally solidified were cut in the longitudinal direction, which is parallel to both the sample axis and the direction of solidification. After this, samples were polished with sand paper and etched with a solution containing 320 ml HCl, 160 ml HNO_3 and 20 ml HF. Etching was performed at room temperature [5]. The position of the CET was located by visual observation and optical microscopy (see black vertical lines in Figure 3 (a), (b) and (c)), and the distance from the bottom of the sample was measured with a ruler.

Results

Typical columnar – to – equiaxed transitions can be observed in Figure 3 for the three samples solidified. The CET occurred in the sample obtained with high velocity of heat extraction at 7.9 cm (CET_{MIN}) to 9.5 cm (CET_{MAX}), at 2.5 cm (CET_{MIN}) to 4.9 cm (CET_{MAX}) in the case of average heat extraction and at 1.5 cm (CET_{MIN}) to 3.6 cm (CET_{MAX}) for low heat extraction from the base of the sample.

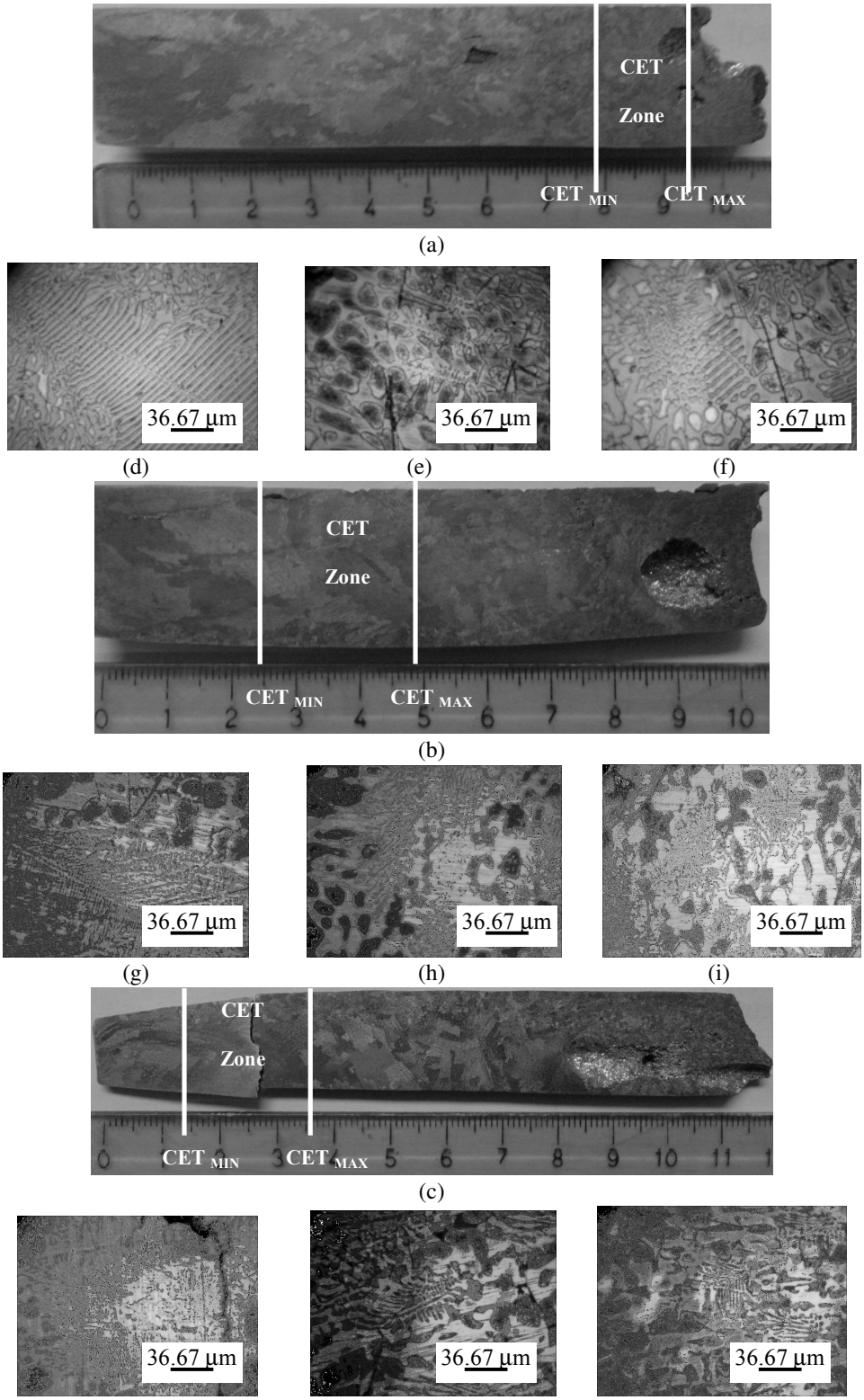

Figure 3. Macrostructures of Al-Cu eutectic alloys corresponding to different velocities of heat extraction: (a) high, (b) average and (c) low and corresponding microstructures in different zones (columnar, CET and equiaxed) of the samples.

In Figure 3 it is clearly seen, as was observed in dendritic Al-Cu alloys [5] that the CET do not occur sharply but in a region of 1 cm or more between the minimum position of the CET ($CET_{MIN.}$) and the maximum position of the CET ($CET_{MAX.}$), see the positions of white vertical lines in Figure 2 (a), (b) and (c). It is highlighted that no effect of the set of the thermocouples in the CET was observed; either acting as nucleating sites or changing the solidification structure.

A typical time dependent temperature plot for all the thermocouples in samples with CET is shown in Figures 4.
The thermocouple T_1 is at the lowest position and the first to reach the solidification front and T_6 is at the highest position. In all the curves it is possible to identify a period corresponding to the cooling of the melt, a second period of solidification and the final period of cooling of the solid to ambient temperature. In some particular cases it is possible to identify a short period of recalescence, when the columnar-to-equiaxed transition occurs at a given thermocouple position [5].

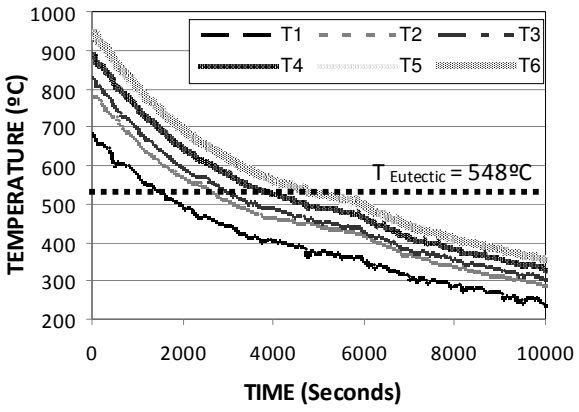

(a)

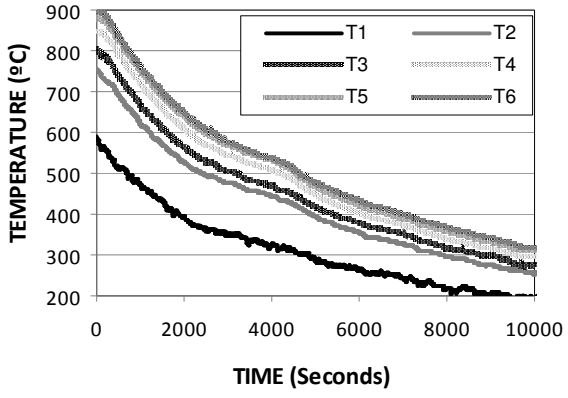

(b)

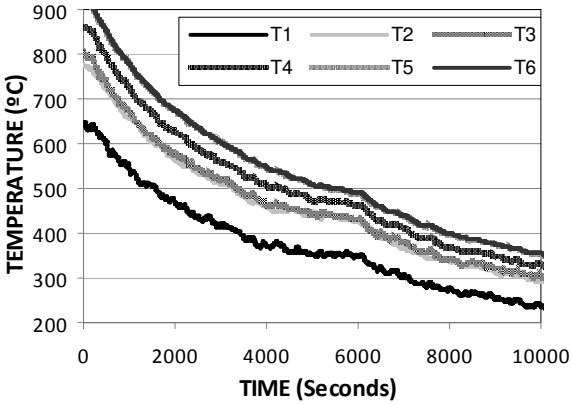

(c)

Figure 4. Temperature versus time curve for (a) high, (b) average and (c) low heat extraction. Al-33.2wt.%Cu.

From the data shown in Figures 4 the following information can be extracted; melt superheat, cooling rate of the melt, position of the solidification fronts for the solidus and the liquidus temperature, local solidification time, velocity of solidification fronts, length of the mushy zone, cooling rate of the solid and temperature gradients.

In some cases the quantification of these parameters is straightforward like the case of melt superheat, which is the highest temperature above the liquidus reached by the melt before the furnace is turned off. It is also the case of cooling rate which is calculated as the slope of the temperature curve in both periods, the cooling of the melt and the solid. The start and the end of solidification at each thermocouple determine the positions of the solidification fronts versus time, which correspond to the experimental liquidus and solidus temperature, respectively. These are not necessarily the liquidus and the solidus temperature from the equilibrium phase diagram. Both points are detected by changes in slopes of the cooling curves at the start and at the end of solidification. This criterion was chosen in order to allow for undercooling to occur before solidification and possible recalescence during solidification of equiaxed grains, since this process is characterized by nucleation and solidification of grains in the melt rather than for what is observed in a normal solidification process where there is a dendrite tip front advancing in the melt. The local solidification time at each thermocouple location is determined by the period of time taken for the temperature going from the liquidus to the solidus temperature.

The velocity of a given solidification front is calculated as the distance between the thermocouples divided by the time taken by either, the liquidus or solidus temperatures to go from the lower to the upper thermocouple.

The cooling rate, T, was determined from the temperature versus the time curves at each thermocouple position and taking the average slope during the cooling of the melt, before a period of solidification. The temperature interval utilized to calculate the slope was between the liquidus temperature and the highest temperature above the liquidus reached by the melt before the furnace was turned off. The values for each experiment are 0.036 ºC/s, 0.042 ºC/s and 0.059 ºC/s.

The temperature gradients at all times are calculated straightforward, dividing the temperature difference between two thermocouples by the separation distance between them.
The values of gradients are plotted in Figure 5 (a to c) for three experiments, and for each alloy. In all figures it is observed that from the beginning of solidification, the gradients decrease with time. The minimum value always corresponds to the position of the columnar-to-equiaxed transition. The critical temperature gradients (at the moment of the CET) are 2.1 °C/cm, 0.1 °C/cm and –4.3 °C/cm for high, average and low heat extraction from the base of the sample, respectively. The critical gradient determined is negative for the experiment with low heat extraction. This negative value is an indication of a reversal in the temperatures profiles ahead of the interface, which could be associated to the recalescence due to massive nucleation of equiaxed grains, and previously reported and discussed for dendritic alloys [5]. The fact that in some cases the position of the thermocouples are not located at the precise position where the CET occurs, may prevent detection of the negative gradients which is believe to occur in all cases. Nevertheless, the values always reach a minimum value at this position. Values of 10 to 60 °C/cm are observed at the beginning of solidification (columnar structure) and when the structure is equiaxed the values of the gradient are around 5 to 10 °C/cm.

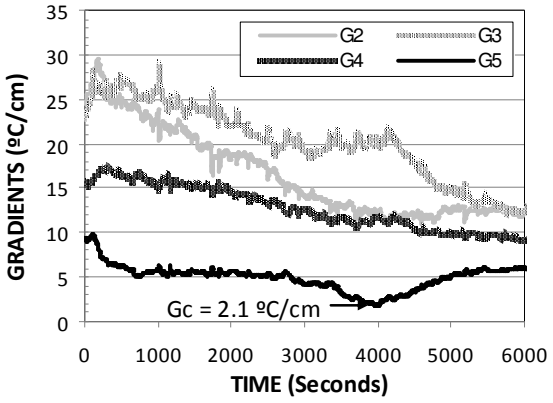

(a)

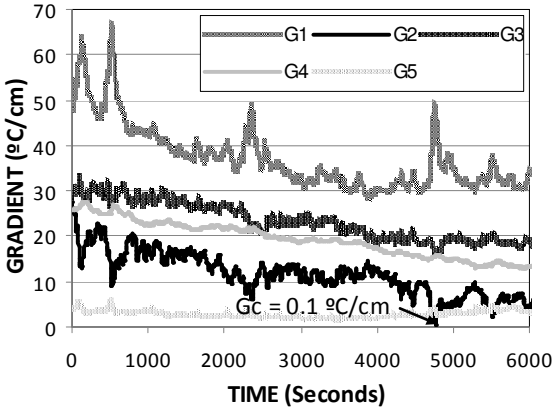

(b)

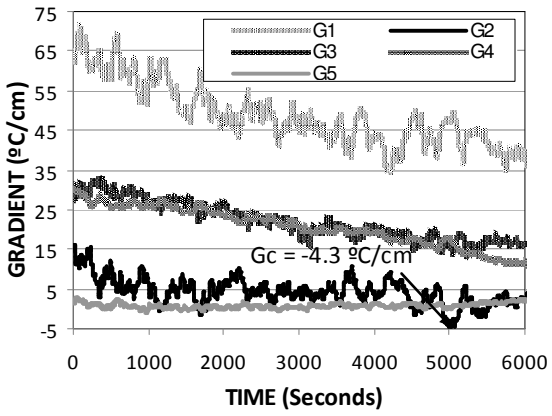

(c)

Figure 5. Temperature gradients versus time for (a) high, (b) average and (c) low heat extraction. Al-33.2wt.%Cu.

Lamellar spacing, λ , was measured in different zones along the samples of Al-33.2wt.%Cu, as can be seen in Figure 6.

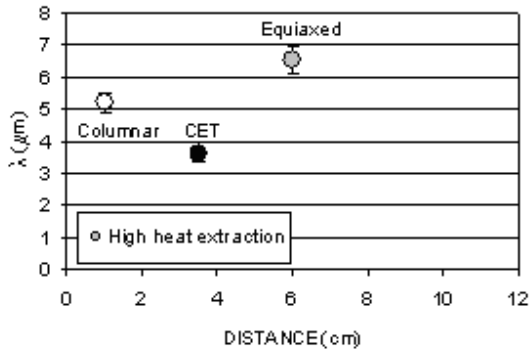

Figure 6. Lamellar spacing, λ, versus distance from the base of the sample.

It is possible to appreciate that the λ spacing increases from the base (columnar zone) to the top of the sample (equiaxed zone), but in the CET zone the λ spacing is small. Similar behavior follows grain size from the bottom to the top of the sample. Otherwise, in the CET zone the size of the equiaxed grains are small due to the nucleation and growth in front of the interface, see Figure 7.

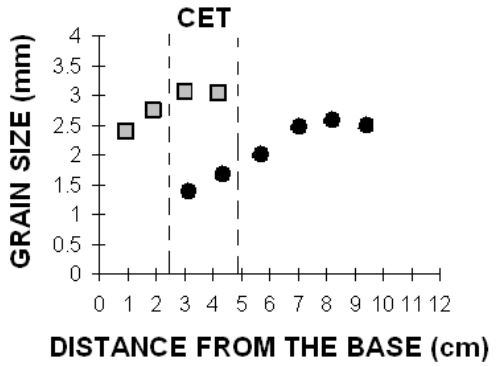

Figure 7. Grain size versus distance.

In Figure 8 the lamellar spacing, λ , was correlated with grow rate or velocity of liquidus front, v. In this figure the red dots correspond to the experimental values themselves, and the other points correspond to the values obtained by other authors in the same alloy system [5, 16-19].

The experimental values are adjusted using the equation:

$$\lambda = 0.1336 \quad v^{-0.5002} \qquad (6)$$

Whereas, the experimental values obtained by Moore and Elliot [16], Cooksey et al. [17], Chadwick [18] and Livingston et al. [19], are adjusted by the equation:

$$\lambda = 0.1283 \quad v^{-0.438} \qquad (7)$$

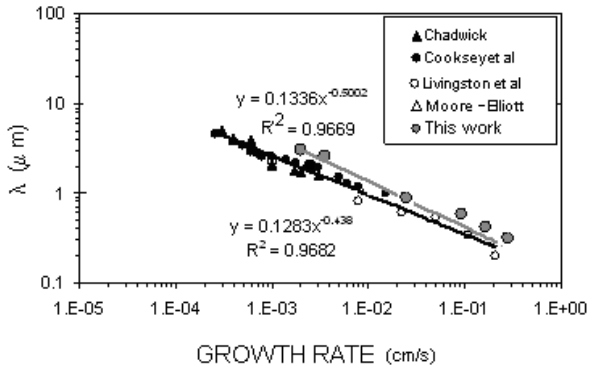

Figure 8. Lamellar spacing, λ, versus growth rate.

Summary and Conclusions

From the results and discussion of the previous sections the main conclusions of this investigation on the correlation between different parameters on the columnar to equiaxed transition in Al-Cu eutectic alloys are:

1. Al-Cu eutectic alloys with CET zone and with different velocities of heat extraction were obtained.
2. The temperature gradient reaches critical values at the CET.
3. The grain size is smaller at the CET region and then beginning to increases until the upper zone of the sample is reached.
4. In the equiaxed region of the samples, the grain size increases monotonically with the size of the spacing.
5. Al-Cu alloys of eutectic alloys were directionally solidified and resulting microstructures were examined. Found that the lamellar spacing varies with the growth rate by the equation $\lambda = 0.1336 \quad v^{-0.5002}$.

Acknowledgements

The authors would like to thanks CONICET for the financial support.
Thanks are given to Ms. Sc. Carlos M. Rodriguez for his collaboration until 07/03/2013.

References

1. J.A. Spittle, Materials Reviews 51 (4) (2006) 247–269.
2. Ch.A. Gandin, ISIJ International 40 (2000) 971–979.
3. D.J. Browne, ISIJ International 45 (2005) 37–44.
4. J.D. Hunt, Materials Science and Engineering 65 (1984) 75–78.
5. A.E. Ares, C.E. Schvezov, Journal of Crystals Growth 312 (2010) 2154–2170.
6. R.Trivedi, Kurz, W., Theory of Dendritic Growth During The Directional Solidification of Binary Alloys, International Materials Reviews, 39, 49 (1994).
7. J.D. Hunt, The Metals Society, London, 3 (1979).
8. W., Kurz, Fisher, D.J., Acta Met. 29, 11 (1981).
9. R. Trivedi, Met. Trans., 15, 977 (1984).
10. J.S. Langer, Muller-Krumbahar, H., Acta Metall., 26, 1689-1695 (1978).
11. R. Elliott, Eutectic Solidification, Int. Met. Reviews, 219, 161 (1977).
12. K.A. Jackson, J.D. Hunt, Lamellar and Rod Eutectic Growth, Trans. AIME, 236, 1129 (1966).
13. J.S. Langer, Eutectic solidification and Marginal Stability, Physical Review Letters, 44, 1023 (1980).
14. R. Trivedi, P. Magnim, W. Kurz, Theory of Eutectic Growth Under Rapid Solidification Conditions, Acta Metall., 35, 971 (1987).
15. M.J. Aziz, Model for Solute Redistribution During Rapid Solidification, J. Appl. Phys., 53, 1158, (1982).
16. A. Moore, R. Elliott, Solidification of Metals, Iron and Steels Institute (1969).
17. D.J.S. Cooksey, D. Munson, M.P. Wilkinson, A. Hellawell, Phil. Mag., 10, 745 (1964).
18. G.A. Chadwick, J. Inst. Metals, 92, 18 (1963-64).
19. J.D. Livingston, H.D. Cline, Trans. Metals Soc. AIME, 245, 351 (1969).